

Communications

Optimization of a Molecular-Based Magnet
MnCu(pbaOH)(H₂O)₃ (pbaOH =
2-Hydroxy-1,3-propanediylbis(oxamato)) with T_c = 30 K

Three years ago, we reported on the design of a molecular-based compound exhibiting a spontaneous magnetization¹ below T_c = 4.6 K. Its formula is MnCu(pbaOH)(H₂O)₃ (**1**) with pbaOH standing for 2-hydroxy-1,3-propanediylbis(oxamato). This compound is one of the few molecular-based magnets described so far.²⁻⁶ **1** was prepared through the reaction of Mn(II) with the copper(II) precursor Cu(pbaOH)₂⁻. Its structure recalled in Figure 1 consists of alternating bimetallic chains assembled within the crystal lattice in such a way that along the *a* direction perpendicular to the chain axis the shortest interchain separations are Mn...Cu instead of Mn...Mn and Cu...Cu. The strategy is reminiscent of an idea put forward by McConnell as early as 1963. The overall ferromagnetic coupling between the ferrimagnetic chains occurs through the interaction between strong positive spin densities belonging to one of the chains and weak negative spin densities belonging to the neighboring chain.⁷ These positive and negative spin densities are provided by the S_{Mn} = 5/2 and S_{Cu} = 1/2 local spins, respectively. The Mn(II)-Cu(II) interaction through the oxamato bridge is indeed strongly antiferromagnetic. This interpretation is substantiated by the fact that MnCu(pba)(H₂O)₃·2H₂O (**2**) with pba standing for 1,3-propanediylbis(oxamato) does not order ferromagnetically.⁸ In **2**, along both the *a* and *b* directions perpendicular to the chain axis the shortest interchain separations are Mn...Mn and Cu...Cu. The differences of topology between **1** and **2** are schematized as follows:⁹

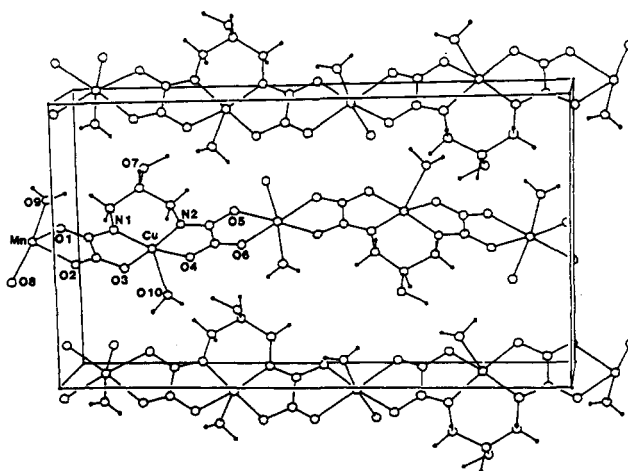
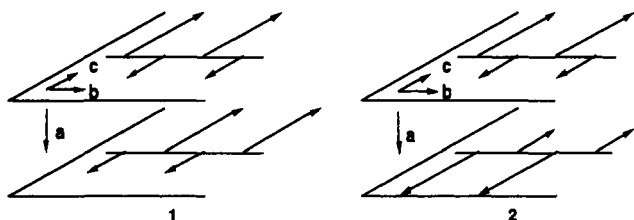


Figure 1. Structure of the crystal lattice for MnCu(pbaOH)(H₂O)₃ (**1**). The *a* axis runs top to bottom, and the *b* axis, left to right.

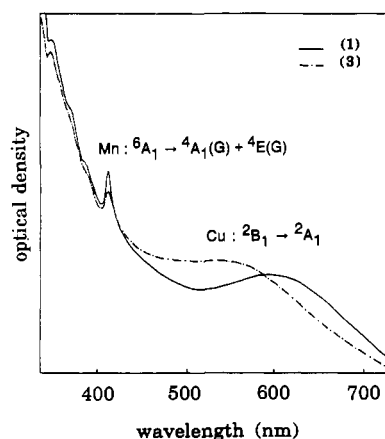


Figure 2. Comparison of the electronic absorption spectra for MnCu(pbaOH)(H₂O)₃ (**1**) and MnCu(pbaOH)(H₂O)₂ (**2**). The spectra are obtained in Nujol mulls.

The T_c = 4.6 K value for **1** immediately raises the following question: Is it possible to shift T_c toward higher temperatures? In this communication, we describe what we have done along this line.

In the mean-field approximation, T_c is related to the intrachain J_{intra} and interchain J_{inter} exchange parameters through¹⁰

$$kT_c = S^2(J_{\text{intra}}J_{\text{inter}})^{1/2} \quad (1)$$

(9) It has been found from magnetic anisotropy measurements and a single-crystal EPR investigation that the preferred spin orientation was along the *c* axis. See: Gatteschi, D.; Guillou, O.; Zanchini, C.; Sessoli, R.; Kahn, O.; Verdager, M.; Pei, Y. *Inorg. Chem.* **1989**, *28*, 287.

- (1) Kahn, O.; Pei, Y.; Verdager, M.; Renard, J. P.; Sletten, J. J. *Am. Chem. Soc.* **1988**, *110*, 782.
- (2) Miller, J. S.; Calabrese, J. C.; Rommelmann, H.; Chittipeddi, S. R.; Zhang, J. H.; Reiff, W. M.; Epstein, A. J. *J. Am. Chem. Soc.* **1987**, *109*, 769.
- (3) Nakatani, K.; Carriat, J. Y.; Journaux, Y.; Kahn, O.; Lloret, F.; Renard, J. P.; Pei, Y.; Sletten, J.; Verdager, M. *J. Am. Chem. Soc.* **1989**, *111*, 5739.
- (4) Caneschi, A.; Gatteschi, D.; Sessoli, R.; Rey, P. *Acc. Chem. Res.* **1989**, *22*, 392.
- (5) Broderick, W. E.; Thomson, J. A.; Day, E. P.; Hoffman, B. M. *Science* **1990**, *249*, 401.
- (6) Zhong, Z. J.; Matsumoto, N.; Okawa, H.; Kida, S. *Chem. Lett.* **1990**, 87.
- (7) McConnell, H. M. *J. Chem. Phys.* **1963**, *39*, 1910.
- (8) Pei, Y.; Verdager, M.; Kahn, O.; Sletten, J.; Renard, J. P. *Inorg. Chem.* **1987**, *26*, 138.

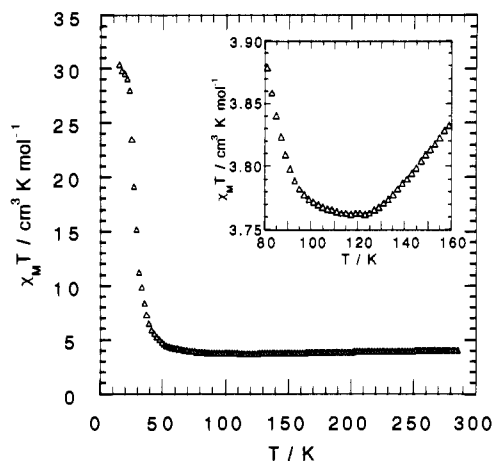


Figure 3. $\chi_M T$ versus T plot for 3.

where S denotes here $S_{Mn} - S_{Cu} = 2$. J_{intra} is directly governed by the nature of the bridge and cannot be modified without changing the copper(II) precursor used in the synthesis. As for J_{inter} , it might well be related to the interchain separations, since there is no obvious exchange pathway connecting the chains. A careful examination of the structure of **1** (see Figure 1) suggests that this separation along the a axis is partially controlled by the water molecule in apical position weakly bound to copper ($Cu-O = 2.417 \text{ \AA}$). It follows that if this molecule was selectively removed, the chains might be closer to each other and J_{inter} increased to some extent.

Warming **1** in the solid phase at $100 \text{ }^\circ\text{C}$ under vacuum for 48 h affords a new compound of formula¹¹ $MnCu(pbaOH)(H_2O)_2$ (**3**). The comparison of the electronic absorption spectra for **1** and **3** in Figure 2 reveals that the water molecule removed belonged to the $Cu(II)$ coordination sphere in **1**. Indeed, the $Cu(II)$ $d-d$ band (${}^2B_1 \rightarrow {}^2A_1$ assuming a C_{4v} symmetry) is shifted from 590 nm in **1** to 555 nm in **3**, as expected when the change is made from a square-pyramidal to a square-planar environment.¹² On the other hand, the energy of the $Mn(II)$ spin-forbidden transition (${}^6A_1 \rightarrow {}^4A_1(G) + {}^4E(G)$ assuming an O symmetry) activated by an exchange mechanism is quasiunchanged (410 nm in **1** and 409 nm in **3**), confirming that the $Mn(II)$ coordination spheres are similar in **1** and **3**.

The $\chi_M T$ versus T plot¹³ for **3**, χ_M being the molar magnetic susceptibility and T the temperature, shows the minimum characteristic of one-dimensional ferrimagnetic behavior at 120 K (see Figure 3). Actually, **3** behaves magnetically exactly like **1** down to 50 K, indicating that the chain structure is retained and that J_{intra} keeps the same value (-23.4 cm^{-1}) in both compounds. On the other hand, when T is lowered below 50 K, $\chi_M T$ for **3** increases much more rapidly than for **1**. The ratio $(\chi_M T)_3/(\chi_M T)_1$ is enhanced from 1 to 3 between 50 and 30 K.¹⁴ This indicates that the spin correlation is much more pronounced in the partially dehydrated compound. This correlation occurs not only along the chain but between the chains as well. The magnetization M versus T curves¹³ for **3** are shown in Figure 4. The field-cooled magnetization (FCM) measured in cooling down within a field of 5 G shows a rapid increase of M below ca. 35 K and then a break at 30 K. The zero-field cooled magnetization (ZFCM)

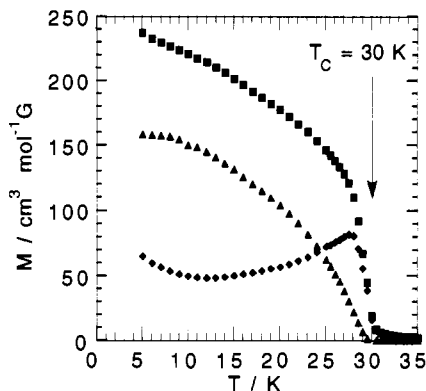


Figure 4. Temperature dependences of the magnetization for $MnCu(pbaOH)(H_2O)_2$ (**3**): (■) FCM; (◆) ZFCM; (▲) RM.

measured in cooling in zero field down to 5 K and then warming up within the field of 5 G shows a maximum just below 30 K. Finally, the remnant magnetization (RM), obtained in switching off the field at 5 K and warming up in zero field, vanishes at 30 K. These three curves reveal that **3** orders magnetically at $T_c = 30 \text{ K}$. At this temperature the slope of the ZFCM versus T curve is maximum. Below T_c the variation of M as a function of the field H (up to 8 T) is typical of what is expected for a powder magnetic material with a very large zero-field susceptibility and then a rapid saturation.¹⁴ The saturation magnetization is $M_S = 22.3 \times 10^3 \text{ cm}^3 \text{ G mol}^{-1}$ (or $4 \mu_B \text{ mol}^{-1}$, μ_B being the Bohr magneton), which confirms that all the $Mn(II)$ spins are aligned along the same direction and the $Cu(II)$ spins along the opposite direction. The M versus H curve¹⁴ presents the same type of hysteresis as what has been reported for **1**, with a coercive field of 60 G at 4.2 K.

Through a mild thermal treatment, we succeeded in shifting T_c from 4.6 to 30 K, apparently a record in the area of the molecular-based magnetic materials. Since J_{intra} has not been modified, J_{inter} may be estimated to have been enhanced by a factor of 40 from eq 1. It is worth mentioning that the same thermal treatment does not give the same effect on **2**. The structural topology of the starting compound plays an essential role.

Acknowledgment. We express our deepest gratitude to the Société Nationale Elf Aquitaine, which has financially supported this work and offered a research grant to K.N.

Supplementary Material Available: Figures showing the temperature dependence of the ratio $(\chi_M T)_3/(\chi_M T)_1$ (Figure S5), M versus H curve at 4.2 K and up to 8 T (Figure S6), and M versus H hysteresis loop at 4.2 K (Figure S7) (4 pages). Ordering information is given on any current masthead page.

Laboratoire de Chimie Inorganique
URA No. 420
Université de Paris-Sud
91405 Orsay, France

Keitaro Nakatani
Pierre Bergerat
Epiphane Codjovi
Corine Mathonière
Yu Pei
Olivier Kahn*

Received March 14, 1991

(10) Richards, P. M. *Phys. Rev. B* 1974, 10, 4687.

(11) Anal. Calcd for $C_7H_{10}N_2O_9CuMn$ (**3**): C, 21.86; H, 2.62; N, 7.28; Cu, 16.52; Mn, 14.28. Found: C, 21.76; H, 2.51; N, 7.36; Cu, 16.59; Mn, 14.08.

(12) Nakatani, K.; Pei, Y.; Mathonière, C.; Kahn, O. *New J. Chem.* 1990, 14, 861.

(13) The magnetic susceptibility measurements were carried out with a Faraday type magnetometer, and the magnetization measurements with a Métrologie-Ingénierie SQUID magnetometer working in both low-field (a few gauss) and high-field (up to 8 T) modes. The magnetic susceptibility data of Figure 3 were measured within a magnetic field of 10^3 G . Those data were corrected for background and core diamagnetism.

(14) Supplementary material.

The Lithium Chloride Adduct of Monolithiated 5,10-Dihydrophenazine: $[Li_2(\mu-Cl)(\mu-NC_{12}H_8NH)(THF)_4]$

The high polarity of Li–N bonds causes lithium amides to associate,¹ yielding dimers or higher oligomers, depending on the size of the substituents on the N-center and the degree of solvation of lithium.^{2–5} Only for exceptionally bulky amides and/or

(1) Setzer, W. N.; Schleyer, P. v. R. *Adv. Organomet. Chem.* 1985, 24, 353.

(2) Engelhardt, L. M.; Jacobsen, G. E.; Junk, P. C.; Raston, C. L.; Skelton, B. W.; White, A. H. *J. Chem. Soc., Dalton Trans.* 1988, 1011 and references therein.